JOURNAL OF PROPULSION AND POWER
Vol. 9, No. 3, May–June 1993

Study on Vortex Generator Flow Control for the Management of Inlet Distortion

Bernhard H. Anderson*
NASA Lewis Research Center, Cleveland, Ohio 44135
and
James Gibb†
Defense Research Agency, Bedford, England, United Kingdom

The present study demonstrates that the reduced Navier-Stokes RNS3D code can be used very effectively to develop a vortex generator installation to minimize the engine face circumferential distortion by controlling secondary flow. The computing times required are small enough that studies such as this are feasible within an analysis-design environment with all its constraints of time and costs. This research study also established the nature of the performance improvements that can be realized with vortex flow control, and suggests a set of aerodynamic properties (called observations) that can be used to arrive at a successful vortex generator installation design. This study also indicated that scaling between flight and typical wind-tunnel test conditions is possible only within a very narrow range of generator configurations close to an optimum installation. Lastly, this study indicated that vortex generator installation design for inlet ducts is more complex than simply satisfying the requirement of attached flow, it must satisfy the requirement of minimum engine face distortion.

Nomenclature

A_i = inlet throat area
C_f = wall skin friction coefficient
c = generator chord length
c_1 = decay constant defined by Eq. (3)
DC_{60} = distortion descriptor defined as the maximum $(Pt_{ave} - Pt_{min})/q_{ave}$ in any 60.0 deg sector
D_i = inlet throat diameter
d = lateral spacing between generator blades
h = generator blade height
L = length of inlet duct
M_i = inlet throat Mach number
n_{vg} = number of vortex generator pairs
Pt_{ave} = average total pressure at the engine face
Pt_{min} = minimum total pressure at engine face in any sector of extent 60.0 deg
Pt_0 = freestream total pressure
q_{ave} = average dynamic pressure at the engine face
R_{ef} = engine face radius
Rey = Reynolds number based on throat diameter
R_i = inlet throat radius
r = distance between field point and generator tip
Tt_0 = freestream total temperature
u = flow velocity at generator tip
X, Y, Z = primary Cartesian coordinates
X_{cl}, Y_{cl}, Z_{cl} = Cartesian coordinates along inlet centerline
X_{vg} = axial location of generator sector region
α = aerodynamic angle of incidence, rad
α_{vg} = generator spacing angle
β_{vg} = vane angle-of-incidence
Γ_p = vortex strength at field point in cross section, defined by Eq. (1)
Γ_0 = vortex strength at tip of generator, defined by Eq. (2)
ΔPt = total pressure loss of vortex generators
δ = boundary-layer thickness
θ_s = generator sector angle
ρ = fluid density

Received April 30, 1992; presented as Paper 92-3177 at the AIAA/ASME/SAE 28th Joint Propulsion Conference, Nashville, TN, July 6–7, 1992; revision received Oct. 26, 1992; accepted for publication Nov. 13, 1992.

*Senior Research Scientist. Member AIAA.
†Senior Engineer.

Introduction

MODERN tactical aircraft are required to be maneuverable at subsonic, transonic, and supersonic speeds, and have good cruise performance. Consequently, proper integration of the engine inlet with the airframe is of paramount importance. Regarding performance and operation, design for optimum airframe-inlet integration has the following goals: 1) to minimize approach flow angularity with respect to the inlet cowl lip; 2) to deliver uniform, high-pressure recovery flow to the inlet face; 3) to prevent or minimize vortex, wake, and boundary-layer ingestion by the inlet throughout the flight envelope; 4) to reduce foreign object damage (FOD)/hot gas ingestion by the inlet; and finally 5) to minimize the potential for flowfield interference from weapon carriage/firing, landing gear deployment, tanks, pods, or other hardware. The combination of inlet design and airframe integration must not only provide high-pressure recovery to maintain the desired thrust levels, but also generate low-flow distortion consistent with stable engine operation.

Engine face flow distortion is one of the most troublesome and least understood problems for designers of modern inlet engine systems.[1,2] One issue is that there are numerous sources of distortion that are either ingested by the inlet or generated within the inlet duct itself. Among these sources are: 1) flow separation at the cowl lip during maneuvering flight; 2) flow separation on the compression surfaces due to shock-wave boundary-layer interactions; 3) spillage of the fuselage boundary layer into the inlet duct; 4) ingestion of aircraft vortices and wakes emanating from upstream disturbances; and 5) secondary flow and possibly flow separation within the inlet duct itself. Most aircraft have experienced one or more of these types of problems during development, particularly at high Mach numbers and/or extreme maneuver conditions, such that flow distortion at the engine face exceeded allowable surge limits. Such compatibility problems were encountered in the early versions of the B70, the F-111, the F-14, the MIG-

25, the Tornado, and the Airbus A300 to name a few examples.

One of the most commonly used methods to control local boundary-layer separation within diffusing ducts is the placement of vortex generators upstream of a problem area. Vortex generators in use today are small wing sections mounted on the inside surface of the inlet inclined at an angle to the oncoming flow to generate a shed vortex. The generators are usually sized to the local boundary-layer height for the best interaction between the shed vortex and boundary layer, and are usually placed in groups of two or more upstream of a problem area. Flow control using vortex generators traditionally relies on induced mixing between the high-energy core stream and the low-energy boundary layer to energize the boundary layer in order to inhibit flow separation.

It was not until the confirmation test by Kaldschmidt et al.[3] on the 727 center inlet for the refanned JT8D engine that an attempt was made to use vortex generators to restructure the development of secondary flow in order to improve the engine face distortion level. With this work, a very important shift in strategy on the use of vortex generators had occurred. The perspective had moved from a local one, in which the goal was to prevent boundary-layer separation, to a global one, in which the goal was to manage secondary flow in order to minimize engine face distortion. However, in order to effectively accomplish this new goal, the design strategy must shift from an experimental- to an analysis-based methodology because of the high costs associated with experimental parametric studies.

The overall goals of this study are to advance the understanding, the prediction, and the control of inlet distortion, and to study the basic interactions that are involved in the management of secondary flows within inlet ducts using computational fluid dynamics (CFD). This article examines the central question as to whether judgments about vortex generator installations optimized for flight conditions can be drawn from scaled wind-tunnel test results, and it studies the aerodynamic properties of engine face distortion and its control over a wide range of flow conditions. Specific objectives of this article are 1) to demonstrate the capability of the reduced Navier-Stokes code RNS3D to design a vortex generator system for the M2129 inlet S-duct, which will be tested over a wide range of conditions, including angle-of-incidence and angle-of-yaw; 2) to investigate the similarities and differences between designing and testing generator installations for flight as compared to scaled wind-tunnel test conditions; and 3) to make some formal observations concerning the importance of various vortex generator installation parameters in minimizing engine face distortion over a range of flow conditions from typical scaled wind-tunnel test to flight Reynolds numbers.

Theoretical Background

Three-dimensional viscous subsonic flows in complex inlet duct geometries are investigated by a numerical procedure which allows solution by spatial forward-marching integration, utilizing flow approximations from the velocity-decomposition approach of Briley and McDonald.[4,5] The goal of this approach is to achieve a level of approximation that will yield accurate flow predictions, while reducing the labor below that needed to solve the full Navier-Stokes equations. The governing equations for this approach have been given previously for orthogonal coordinates, and the approach has been successfully applied to problems whose geometries can be fitted conveniently with orthogonal coordinate systems. However, geometries encountered in typical subsonic inlet ducts cannot be easily treated using orthogonal coordinates, and this led to an extension of this approach by Levy et al.[6] to treat ducted geometries with nonorthogonal coordinates. In generalizing the geometry formulation, Anderson[7] extended the analysis to cover ducted geometries defined by an externally generated grid-file, such that it allowed for 1) reclustering the existing grid-file, 2) redefining the centerline space curve, and 3) altering the cross-sectional shape and area distribution without returning to the original grid-file. This version of the three-dimensional reduced Navier-Stokes (RNS) computer code is called RNS3D. The turbulence model used in RNS3D is that of McDonald and Camarata[8] which employs an eddy-viscosity formulation for the Reynolds stresses.

Vortex Generator Model

The model for the vortex generators within the RNS analysis takes advantage of the stream function-vorticity formulation of the governing equations. The shed vortex is modeled by introducing a source term into the vorticity equation that is a function of the geometric characteristics of the generators themselves. This source term is introduced at every point in the cross-plane in the form of the following expression:

$$\Gamma_p = \Gamma_0 e^{-(c_1 r^2)} \tag{1}$$

The geometry of the generator is related to the vortex strength at the blade tip through the term defined by

$$\Gamma_0 = 8.0 \rho u c \tanh(\alpha) \tag{2}$$

The decay constant is given by the expression

$$c_1 = 4.0/c^2 \tag{3}$$

This vortex model resembles the one proposed by Squire,[9] except that it neglects the variation of viscosity in the cross-plane.

Results and Discussions

Vortex Generator Design Considerations

An extensive study was undertaken to develop a vortex generator installation for the M2129 inlet S-duct, and to examine the relationship between the important design variables for the purpose of developing an understanding on how best to control inlet distortion. It was established[4] that vortex generator design for the purpose of minimizing engine face distortion depends on the initial conditions, i.e., generator installation design is a point design and all other flow conditions are off-design. Thus, the installed performance achieved over a range of conditions depends on compromises made in the geometry, arrangement, and location of the vortex generators within the inlet duct. For that reason, this article will consider four generator installation designs each based on different objectives. The four generator designs include 1) an optimum vortex generator installation designed for the AGARD test case 3.2 flow conditions; 2) an optimum vortex generator configuration designed for the AGARD test case 3.1 flow conditions; 3) a vortex generator installation optimized for flight conditions; and 4) a generator installation with the same geometry as that optimized for flight conditions, but relocated within the inlet to operate at the test case 3.2 initial conditions. The purpose of the last two generator configurations is to determine whether judgments about generator configurations optimized for flight conditions can be drawn from scaled wind-tunnel tests results. The AGARD test cases 3.1 and 3.2 are considered to be of typical scaled wind-tunnel test results, and are defined by the following.

AGARD Case 3.1 Test and Initial Conditions

Total pressure	$Pt_0 = 29.889$ in./Hg
Total temperature	$Tt_0 = 293$ K
Throat Mach number	$M_i = 0.794$
Throat diameter	$D_i = 5.071$ in.
Throat area	$A_i = 25.254$ in.^{2}
Reynolds number (based on D_i)	$Rey = 1.848 \times 10^6$

AGARD Case 3.2 Test and Initial Conditions

Total pressure	$Pt_0 = 29.865$ in./Hg
Total temperature	$Tt_0 = 293$ K
Throat Mach number	$M_i = 0.412$
Throat diameter	$D_i = 5.071$ in.
Throat area	$A_i = 25.254$ in.^{2}
Reynolds number (based on D_i)	$Rey = 1.158 \times 10^6$

Flight conditions for this study are considered to be M_i of 0.412 and Rey of 8.264×10^6 based on inlet throat diameter.

Installed Vortex Generator Performance Characteristics

The M2129 inlet duct geometry and computational mesh used in this study are shown in Fig. 1, and was based on a study by Willmer et al.[11] The centerline of the inlet defined in terms of the coordinate system shown in Fig. 1 is given by

$$Z_{cl} = -\Delta Z_{cl}\{1 - \cos[\pi(X_{cl}/L)]\} \quad (4)$$

where X_{cl} is the x coordinate of the inlet duct centerline, and ΔZ_{cl} is the centerline offset. The radius distribution measured perpendicular to the duct centerline is given by

$$\left(\frac{R - R_i}{R_{ef} - R_i}\right) = 3\left(1 - \frac{X_{cl}}{L}\right)^4 - 4\left(1 - \frac{X_{cl}}{L}\right)^3 + 1 \quad (5)$$

For the purposes of the calculations, the M2129 S-duct was nondimensionalized with respect to the throat radius, therefore, $R_i = 1.0$, $R_{ef} = 1.183$, $L = 7.10$, and $\Delta Z_{cl} = 2.13$.

A polar grid topology was chosen for the M2129 S-duct which consisted of 49 radial, 49 circumferential, and 121 streamwise nodal points in the half-plane, for a total number of 290,521 grid points. The CPU time was 8.3 min on the CRAY XMP for this computational grid. The large number of mesh points was chosen in order to resolve the small interactions that are characteristic of vortex generator flowfields within the inlet duct. The internal grid was constructed such that the transverse computational plane was perpendicular to the duct centerline. Grid clustering was used in the radial direction in order to redistribute the nodal points to resolve the high shear regions near the wall. The flow in the inlet was considered turbulent throughout. The inflow boundary-layer condition corresponds to a shear layer thickness $\delta/R_i = 0.120$, and were applied 1-diam upstream of the inlet entrance in the constant area extension.

The geometry of the corotating vortex generators used in this study along with the nomenclature used in positioning the individual blades are presented in Figs. 2 and 3. The important geometric design parameters include 1) the vortex generator blade height h/R_i, 2) the blade chord length c/R_i, and 3) the vane angle-of-attack β_{vg}. Instead of the usual spacing parameter d/R_i, i.e., the distance between adjacent blades, the positioning of the vortex generator blades was described in terms of a lateral α_{vg} and a sector angle over which the blades were positioned θ_s. For this study, the relationship between blade α_{vg} and θ_s is given by

$$\theta_s = \alpha_{vg}(n_{vg} - \tfrac{1}{2}) \quad (6)$$

Equation (6) was also used to position the individual generator blades around the inside periphery of the inlet duct at a given axial sector location X_{vg}/R_i. The angle θ_s was measured counterclockwise relative to an azimuthal angle of 180 deg with respect to the vertical axis of the duct. It should be remembered that only a half-duct calculation was performed in this study, and Eq. (6) is used to place the individual vortex generators within that half-duct. Thus, the total number of vortex generators within the real inlet is twice the number actually used in the calculation. Also, since the other half of the inlet duct is the mirror image of the computational duct, each corotating generator can be viewed as having a corresponding mirror image, i.e., the corotating vortex generators can be labeled as pairs. Shown in Fig. 4 are the axial locations of the vortex generator sector regions covered in this study. These sector regions were positioned between $X_{vg}/R_i = 1.0$ and $X_{vg}/R_i = 5.0$, and covered θ_s up to 157.5 deg in half-plane computational duct, or 315.0 deg in the real duct.

The standard blade section used in this study was composed of a low-aspect ratio flat-plate vane-type generator, where the ratio of h/c was fixed at 0.259, and β_{vg} was set at 16.0 deg. Although not part of this study, it has been found that the strength of the individual vortex from the generator blade does not vary rapidly with β_{vg} for low-aspect ratio vanes, and so the system is relatively insensitive to changes in local flow

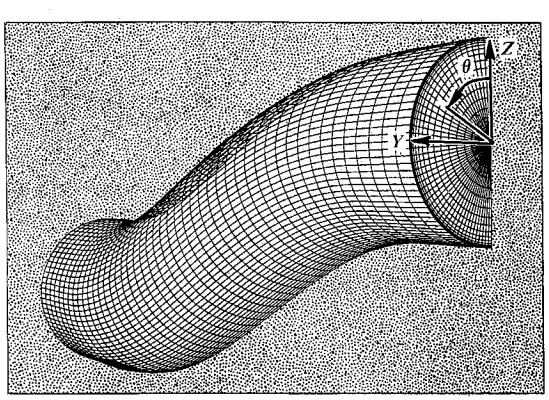

Fig. 1 Geometry definition for the M2129 intake duct.

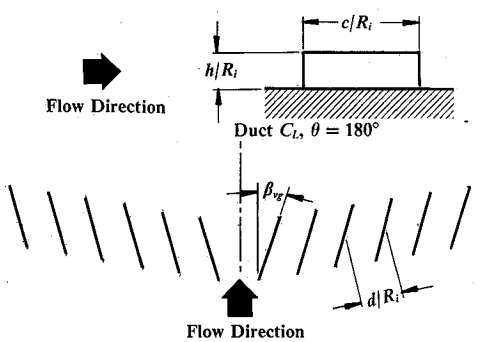

Fig. 2 Geometry definition of corotating vortex generators.

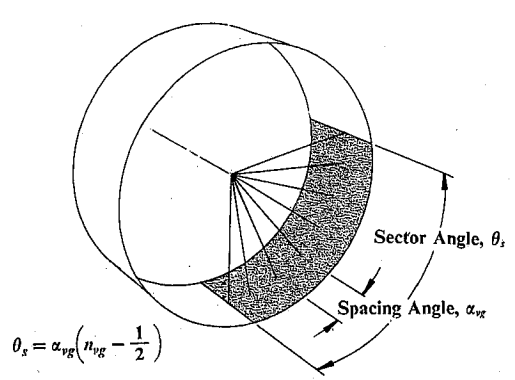

Fig. 3 Nomenclature used for vortex generator positioning.

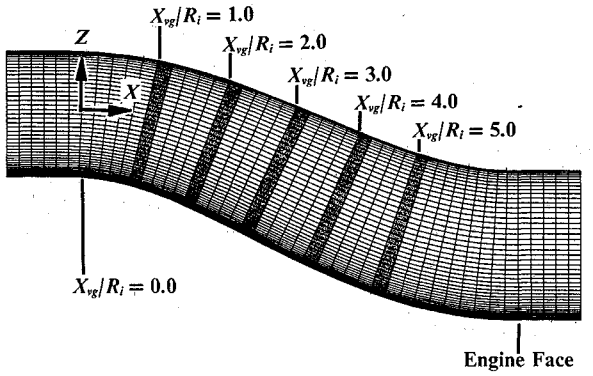

Fig. 4 Axial locations of the vortex generator sector regions.

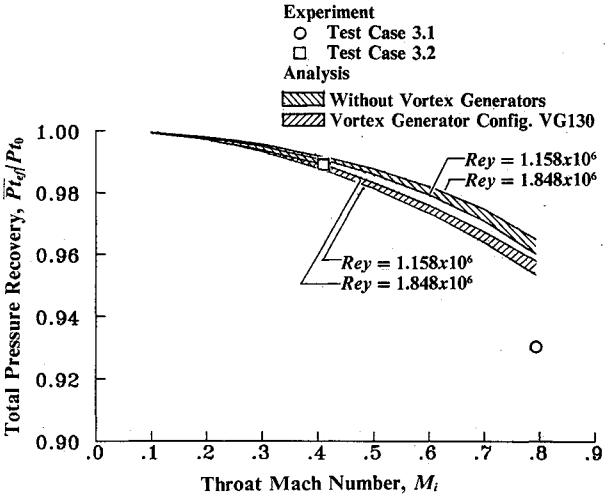

Fig. 5 Effect of vortex flow control on engine face total pressure recovery for the M2129 intake duct and VG130.

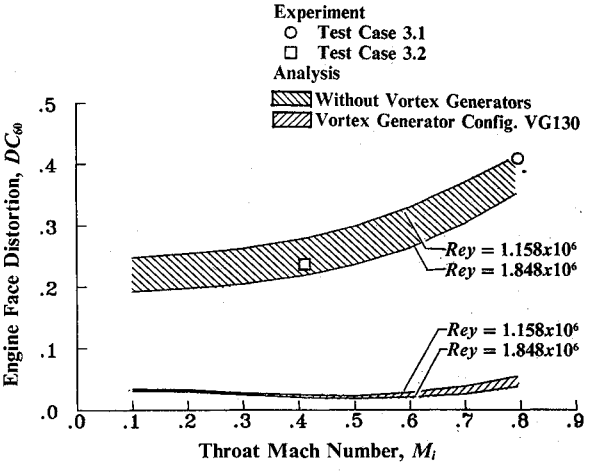

Fig. 6 Effect of vortex flow control on engine face DC_{60} distortion for the M2129 intake duct and VG130.

direction on the surface. This is in agreement with the conclusions reached by Pearcy[12] who obtained his information from experimental measurements.

For comparison with the experimentally measured inlet performance, computations were made at inlet throat Mach numbers of 0.794 and 0.412, and corresponding Reynolds numbers of 1.848×10^6 and 1.158×10^6, based on D_i. These correspond to the AGARD test cases 3.1 and 3.2 initial conditions previously defined. Figures 5 and 6 show a comparison between the measured and calculated engine face total pressure recovery and engine face DC_{60} distortion for the M2129 S-duct inlet without vortex flow control, and with vortex generator configuration VG130 installed in the inlet. Vortex generator installation VG130, which is the configuration optimized for the test case 3.2 initial flow conditions, gave the best overall performance between Mach numbers 0.10–0.80, and is defined by the following.

VG130

Number of corotating generator pairs	$n_{vg} = 11$
Vortex generator sector location	$X_{vg}/R_i = 3.0$
Generator blade height	$h/R_i = 0.075$
Generator chord length	$c/R_i = 0.2896$
Generator spacing angle	$\alpha_{vg} = 15.0$ deg
Generator vane angle of attack	$\beta_{vg} = 16.0$ deg
Generator sector angle	$\theta_s = 157.5$ deg

The theoretical performance is shown in Figs. 5 and 6 as a function of inlet throat Mach number at Reynolds number corresponding to the test case 3.1 and test case 3.2 initial conditions, i.e., $Rey = 1.848 \times 10^6$ and $Rey = 1.158 \times 10^6$, respectively. For the range of inlet throat Mach numbers between 0.412–0.794, the analysis indicated the flow separated, and the separation was that associated with vortex liftoff.[10] The separation (or vortex liftoff) occurring at an inlet Mach number of 0.412 was "weak," and progressively increased in strength as the throat Mach number increased, becoming quite severe at an inlet Mach number of 0.794. RNS3D was able to predict the total pressure recovery for weak separation quite well, but the difference between analysis and measurements become progressively worse as the separation increases in strength, i.e., as its influence on the overall inlet flowfield becomes more pronounced. The overprediction of inlet total pressure recovery at the higher throat Mach numbers could result from the fact that current turbulence models are unable to represent turbulent separation (or vortex liftoff) with sufficient accuracy to predict the separation location. Current turbulence models invariably predict separation further downstream in the inlet duct than is indicated by measurements. The good predictions of the DC_{60} engine face distortion in the higher Mach number range probably resulted from compensating errors, although differences between calculations and measurements will also occur if the data reduction procedures for both computational and experimental information are not exactly the same.

With VG130 installed in the inlet, the flow remains attached over the entire Mach number range considered, affecting a number of important flow properties. First and foremost, VG130 suppressed both the Mach number and Reynolds number influence on the DC_{60} engine face distortion characteristics. Secondly, the level of engine face circumferential distortion was reduced to a very acceptable level over a wide range of inlet throat Mach numbers. Thirdly, as a consequence of the vortex generator installation, an additional total pressure loss occurred as result of mixing between the vortex flow and the main flow within the inlet. These losses are a function of both Mach number and Reynolds number. Thus, a compromise must be made between improved distortion at the engine face as a consequence of vortex generators and a total pressure loss associated with the generator installation.

It is important to indicate that the DC_{60} distortion descriptor has the interesting property that both the numerator (defined by the pressure difference $Pt_{ave} - Pt_{min}$) and the denominator (defined by the average dynamic pressure q_{ave} at the engine face) approach zero as the inlet throat Mach number approaches zero. In addition, in examining inlet throat Mach number effects on DC_{60}, it is important to understand that what is being measured is the change in a pressure difference relative to the average engine face dynamic pressure, both of which decrease with Mach number. The pressure difference

$Pt_{ave} - Pt_{min}$ is affected by inlet throat Mach number in two ways: 1) as a simple compressibility effect, and 2) as changes in the strength and development of secondary flow itself. It is the changes in the strength and development of secondary flow over the flight envelope that is the very heart of understanding inlet distortion.

Generator Influence on Engine Face Flowfield

Presented in Figs. 7–10 are the engine face total pressure recovery maps and secondary flowfield without vortex generators and with VG130 installed in the M2129 inlet duct, for both test cases 3.1 and 3.2 initial conditions. Also shown on these figures are the DC_{60} engine face distortion values, and the engine face total pressure recovery $\overline{Pt}_{ef}/Pt_0$ values. The performance parameters $\overline{Pt}_{ef}/Pt_0$ and DC_{60} were computed using area weighted values from the computational mesh, rather than the rake used in the experiment.

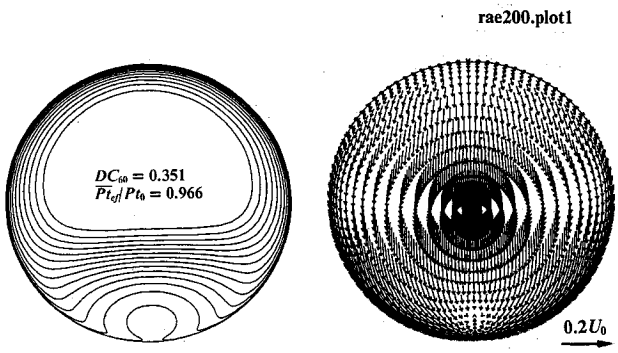

Fig. 7 Engine face flowfield for the M2129 intake duct without vortex generators and test case 3.1 initial conditions.

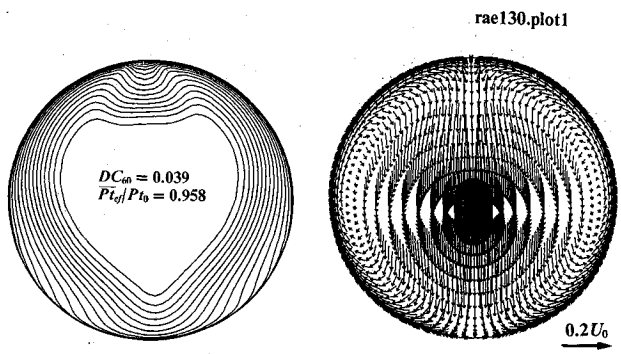

Fig. 8 Engine face flowfield for the M2129 intake duct with VG130 and test case 3.1 initial conditions.

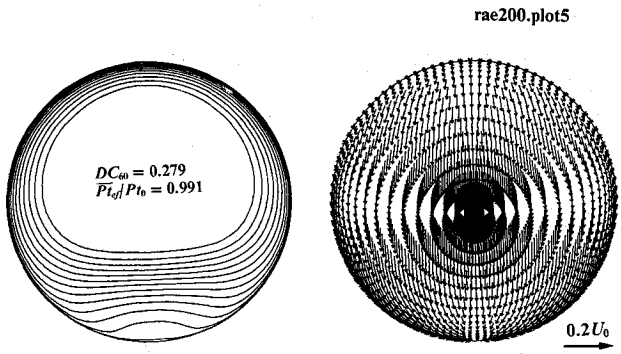

Fig. 9 Engine face flowfield for the M2129 intake duct without vortex generators and test case 3.2 initial conditions.

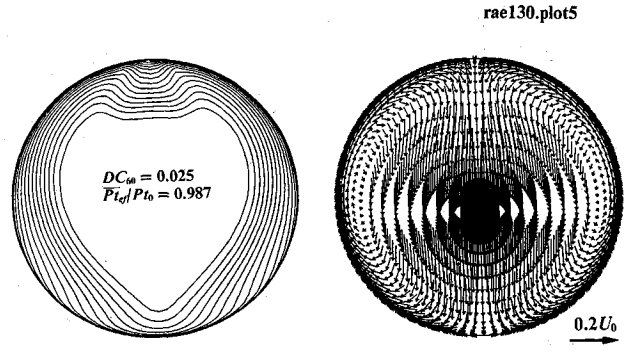

Fig. 10 Engine face flowfield for the M2129 intake duct with VG130 and test case 3.2 initial conditions.

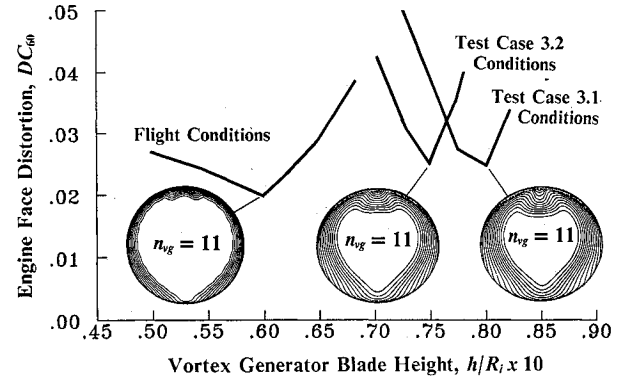

Fig. 11 Effect of vortex generator blade height (h/R_i) on engine face DC_{60} distortion at three inlet initial conditions.

It is evident from these figures that VG130 has the effect of distributing the low-energy flow in a more uniform manner around the inside periphery of the engine face, thus decreasing the DC_{60} engine face distortion substantially. However, the penalty associated with this redistribution process is a decrease in engine face total pressure recovery $\overline{Pt}_{ef}/Pt_0$. The computed total pressure loss $\Delta Pt/Pt_0$ associated with an installation composed of 11 generator pairs is 0.008 at the test case 3.1 initial conditions and 0.004 at the test case 3.2 inlet conditions. Although mixing takes place between the high-energy core flow and low-energy boundary-layer flow, the primary gains result as a consequence of this redistribution process. Thus, vortex flow control of inlet distortion can also be viewed as creating a new secondary flowfield that will redistribute the low-energy flow in a more uniform manner at the engine face station.

Differences Between Flight and Test Performance

Presented in Fig. 11 is the effect of vortex generator blade height h/R_i on engine face DC_{60} distortion at three inlet initial conditions, i.e., flight, test case 3.2, and test case 3.1 initial conditions. The vortex generator installation was composed of 11 pairs of corotating generators located at an axial position $X_{vg}/R_i = 3.0$ with an angular lateral spacing α_{vg} of 15.0 deg between the generator blades. The results presented in Fig. 11 illustrate one of the primary differences between generator installations designed for flight conditions and those which are optimized for wind-tunnel test conditions, i.e., the optimum blade height is smaller at the higher Reynolds numbers that are associated with flight conditions. Comparing test cases 3.2 and 3.1 performance results on Fig. 11 indicates that M_i also plays a role in determining the optimum blade height. Figure 11 indicates the important characteristic that the installed performance degrades much faster at scaled test conditions than at flight conditions, therefore, the choice of blade height becomes a more critical decision at wind-tunnel con-

ditions. In summary, it can be observed from Fig. 11 that, for a given configuration of vortex generators positioned at a fixed axial location, there exists a blade height which will minimize the engine face distortion.

Figure 12 shows the effects of vortex generator sector location X_{vg}/R_i on engine face DC_{60} distortion at the three initial conditions, and corresponding optimum generator blade height h/R_i determined from Fig. 11. The generator installation was again composed of 11 corotating blades using an angular spacing α_{vg} of 15.0 deg. These optimum h/R_i were determined to be 0.060 for flight conditions, 0.075 for the AGARD test case 3.2 condition, and 0.080 for the AGARD test case 3.1 initial conditions. At each of these optimum generator blade heights and test conditions, the location for these installations were all at the same axial location at $X_{vg} = 3.0$. Figure 12 also demonstrates that scaling between flight and wind-tunnel test conditions are possible only in the neighborhood of a vortex generator installation that has been optimized for blade height and sector location, i.e., an optimum generator design. Figure 12 also indicates that the degradation in performance, as the flow conditions move further from that which were used to optimize the vortex generator installation, is much faster under test conditions than at flight conditions. This characteristic can be related to the generator scale effect h/δ (ratio of generator blade height to boundary layer thickness) and is caused by the face that in three-dimensional inlet ducts, the boundary-layer thickness changes more rapidly at the lower Reynolds numbers as a result of the effects of secondary flow. Because of this characteristic, the placement of the generator is more critical at tunnel test conditions than it is at flight conditions, but the following fundamental aerodynamic property is still a valid observation over a wide range of flow conditions. For a given geometry and arrangement of vortex generators, there exists an axial location which will minimize engine face distortion at a given inlet flow condition.

The results indicated in Figs. 11 and 12 define three vortex generator installations: 1) an optimum vortex generator installation designed for the AGARD test case 3.2 flow conditions; 2) an optimum vortex generator configuration designed for the AGARD test case 3.1 flow conditions; and 3) a vortex generator installation optimized for flight conditions. These generator configurations have been labeled VG130, VG230, and VG430, respectively. VG130 has been previously defined, however, configurations VG230 and VG430 are specifically defined as follows.

VG230

Number of corotating generator pairs	$n_{vg} = 11$
Vortex generator sector location	$X_{vg}/R_i = 3.0$
Generator blade height	$h/R_i = 0.080$
Generator chord length	$c/R_i = 0.2896$
Generator spacing angle	$\alpha_{vg} = 15.0$ deg
Generator vane angle of attack	$\beta_{vg} = 16.0$ deg
Generator sector angle	$\theta_s = 157.5$ deg

VG430

Number of corotating generator pairs	$n_{vg} = 11$
Vortex generator sector location	$X_{vg}/R_i = 3.0$
Generator blade height	$h/R_i = 0.060$
Generator chord length	$c/R_i = 0.2896$
Generator spacing angle	$\alpha_{vg} = 15.0$ deg
Generator vane angle of attack	$\beta_{vg} = 16.0$ deg
Generator sector angle	$\theta_s = 157.5$ deg

It is apparent from the discussions of Figs. 11 and 12 that the generator scale h/δ plays a very important role in determining installed vortex generator performance, and also suggests that a generator installation optimized for flight can be relocated within the inlet to give the similar performance as

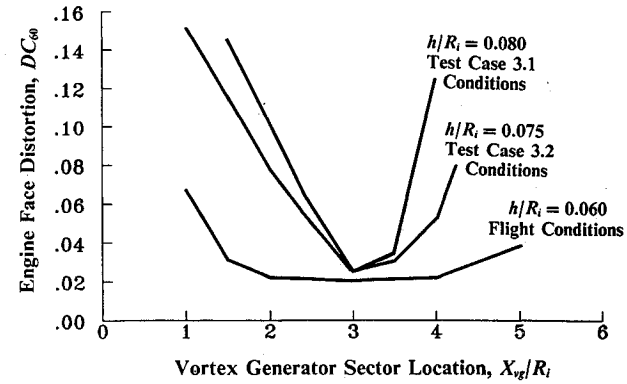

Fig. 12 Effect of vortex generator sector location (X_{vg}/R_i) on engine face DC_{60} distortion at three inlet initial conditions and corresponding optimum generator blade heights (h/R_i).

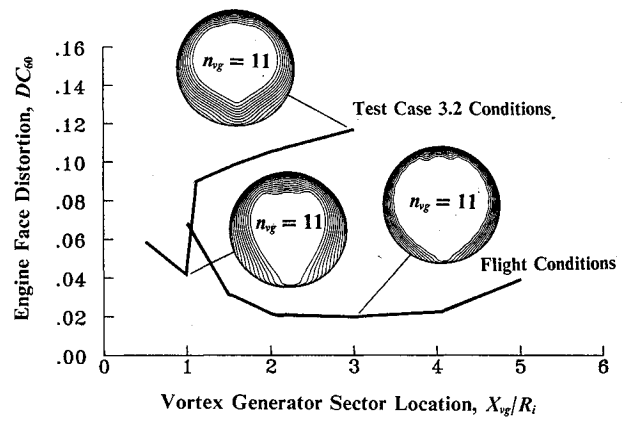

Fig. 13 Effect of vortex generator sector location (X_{vg}/R_i) on engine face DC_{60} distortion, VG430, test case 3.2, and flight conditions.

in scaled wind-tunnel tests. Figure 13 presents the effect of generator sector location X_{vg}/R_i on engine face DC_{60} distortion for VG430 operating both at test case 3.2 and flight conditions. At flight conditions, the optimum axial position for configuration VG430 is at a location $X_{vg}/R_i = 3.0$, and this location provides very low engine face distortion. However, the distortion of this generator configuration at the test case 3.2 conditions is very high. By moving the VG430 configuration forward where the boundary-layer is thinner, the engine face DC_{60} distortion decreases to a more acceptable level. This defines the fourth generator installation in this series, i.e., a generator installation with the same geometry as that optimized for flight conditions, but relocated within the inlet to operate at the test case 3.2 initial conditions. This configuration of corotating vortex generators is defined as follows.

VG310

Number of corotating generator pairs	$n_{vg} = 11$
Vortex generator sector location	$X_{vg}/R_i = 1.0$
Generator blade height	$h/R_i = 0.060$
Generator chord length	$c/R_i = 0.2896$
Generator spacing angle	$\alpha_{vg} = 15.0$ deg
Generator vane angle of attack	$\beta_{vg} = 16.0$ deg
Generator sector angle	$\theta_s = 157.5$ deg

Figure 14 presents the effect of vortex generator sector location X_{vg}/R_i on the engine face DC_{60} distortion with VG430 (defined above) at flight conditions. The total pressure recovery maps shown in Fig. 14 indicates the manner in which the performance changes with axial position, and suggests that this generator installation increases in strength as its location is moved upstream from the optimum position, and decreases

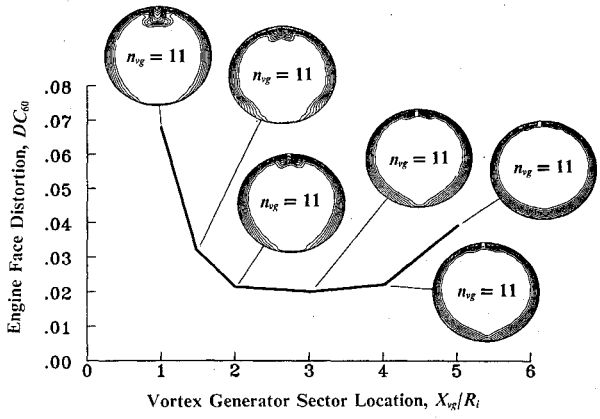

Fig. 14 Effect of vortex generator sector location (X_{vg}/R_i) on engine face DC_{60} distortion, VG430, and flight conditions.

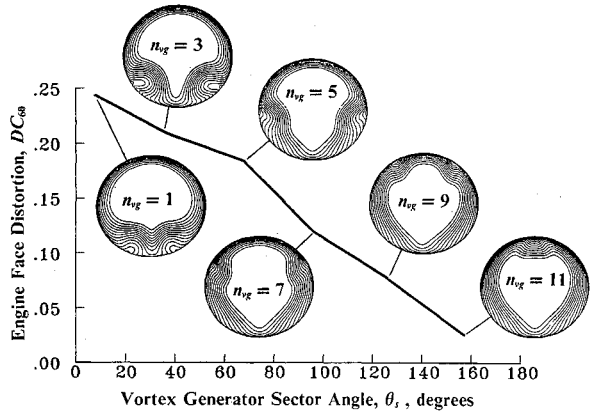

Fig. 15 Effect of vortex θ_s on engine face DC_{60} distortion, VG130 series vortex generators, and test case 3.2 initial conditions.

in strength as the generator installation is moved downstream relative to this optimum location. Under angle-of-incidence or angle-of-yaw conditions, it would be expected that the overall ratio of δ/h to increase, and therefore, a decrease in the overall effectiveness of the generator installation can be expected. However, by moving the generator installation forward of its optimum position, the overall performance at angle-of-incidence and angle-of-yaw can be improved and even optimized, i.e., the aerodynamic properties of vortex flow control that have been discussed are valid at the off-design conditions of angle-of-incidence and angle-of-yaw.

Observations on Vortex Generator Installation Design

The relative engine face distortion levels at different flight conditions is important since inlets must be designed to operate with low distortion over a flight envelope. Trades between what is needed at one flight condition, such as takeoff, and what is needed at other conditions, such as transonic maneuvering at low altitudes or cruise, must be made. Reynolds number, Mach number, inlet mass flow, and engine tolerance can all change from one operating condition to another. Therefore, it is important to understand the influence of these various operating factors, as well as the large number of design parameters associated with the geometry, arrangement, and placement of the generators within the inlet duct. One such geometric parameter identified by Pearcy[12] "as the single most important factor in establishing an effective vortex pattern," for the suppression of flow separation, is the lateral distance between adjacent vortices, i.e., spacing angle in the terminology of this article. However, the spacing angle cannot be examined without first understanding the importance of sector angle in vortex generator design, and these parameters are related in this study according to Eq. (6).

Figure 15 presents the effect of θ_s on DC_{60} for the VG130 series generator configurations at the test case 3.2 initial conditions. Also shown on Fig. 15 are the engine face recovery maps at each of generator sector angles considered in the analysis. As the number of vortex generator pairs increases at a constant spacing angle of 15.0 deg, the sector angle will increase according to Eq. (6). Increasing the number of vortex generators enlarges the sector angle over which the vortex generators are positioned, and this has the effect of "spreading" the low energy flow more evenly around the engine face, and consequently, decreasing the engine face circumferential distortion. Therefore, improved engine face DC_{60} distortion was achieved by increasing the number of generator pairs installed around the inside periphery of the inlet duct. This can clearly be seen from the engine face recovery maps presented in Fig. 15. The penalty associated with increasing the number of vortex generator pairs is a decrease in engine face total pressure recovery. The computed total pressure loss $\Delta Pt/Pt_0$ associated with an installation composed of 11 generator pairs is 0.008 at the test case 3.1 initial conditions and 0.004

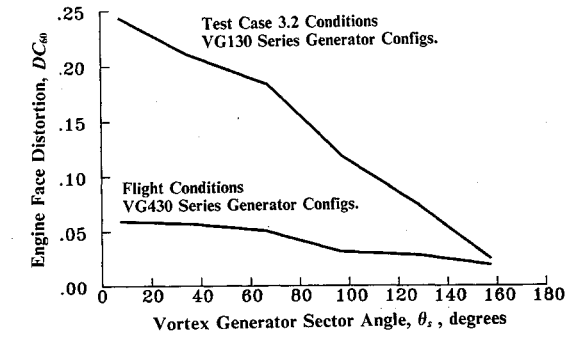

Fig. 16 Effect of vortex θ_s on engine face DC_{60} distortion, VG130 and VG430 series vortex generators, test case 3.2, and flight conditions.

at the test case 3.2 inlet conditions. These results indicate that the losses associated with vortex generator installations is a strong function of Mach number. In summary, it can be observed that the sector angle at which the minimum engine face distortion occurs will be at least 360 deg, although a "local optimum" can occur depending on the chosen distortion descriptor and angle over which the averaging process takes place.

Presented in Fig. 16 is a comparison between the vortex θ_s characteristics for a generator configuration optimized for the test case 3.2 and flight conditions, i.e., VG130 and VG430 series generator configurations, respectively. Similar to characteristics found for h/R_i and installation location X_{vg}/R_i, the choice of "best" θ_s becomes far more critical under test conditions than flight Reynolds numbers. The sector angle characteristics presented in Fig. 16 also suggests that there is a very limited set of installation geometries where scaling between flight and wind tunnel is even possible, and this is in the neighborhood of a best or optimum sector angle.

Having chosen the best sector angle over which the vortex generators are placed, the question arises as to what spacing between generator blades will provide the lowest DC_{60}. Figure 17 presents the effect of vortex α_{vg} on the DC_{60} for a generator installation position at an axial station of 3.0 within the M2129 inlet duct operating at the test case 3.2 initial conditions. Also shown on Fig. 17 are the individual engine face recovery maps at the spacing angles considered in the analysis. For this sequence, the generator sector angle was held fixed at 157.5 deg, while the spacing is determined from Eq. (6) for a given number of vortex generators. The spacing of the individual generator blades around the inside periphery of the inlet duct was also determined from Eq. (6). For this set of inlet flow conditions, vortex generator geometry, installation location, and inlet duct aerodynamic characteristics, there existed a generator spacing angle which minimized the DC_{60} engine face

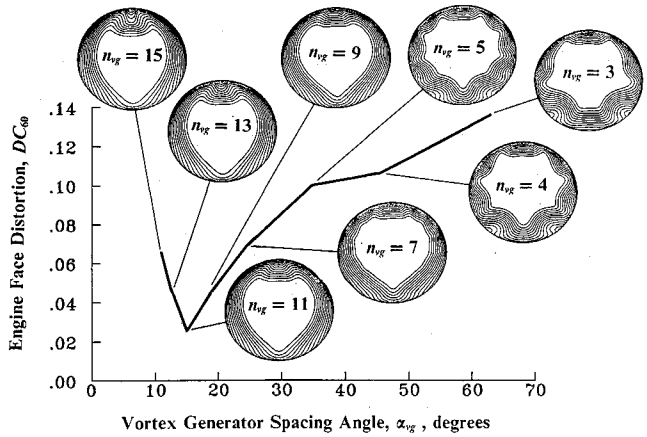

Fig. 17 Effect of vortex α_{vg} on engine face DC_{60} distortion, VG130 series vortex generators, and test case 3.2 initial conditions.

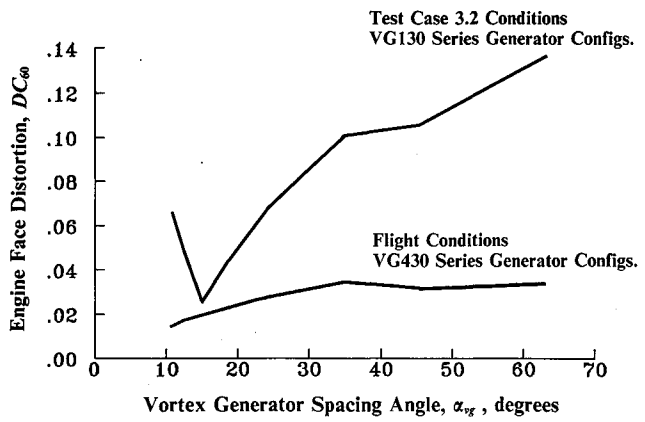

Fig. 18 Effect of vortex α_{vg} on engine face DC_{60} distortion, VG130 and VG430 series vortex generators, test case 3.2, and flight conditions.

circumferential distortion, and this optimum spacing angle was 15.0 deg.

This suggests a different design guideline for vortex generator installations from that recommended by Pearcy,[12] but bear in mind that the effectiveness parameter used in that study was retention of the individual vortex identities downstream of the generator blades as measured on a flat plate, while the effectiveness indicator used in this study is the DC_{60} engine face circumferential distortion descriptor. Increasing the vortex generator spacing angle does indeed increase the retention of the individual vortex identities, as can be seen from the series of engine face total pressure recovery maps presented in Fig. 17, but it does not necessarily lead to a minimum DC_{60}. Thus, with regards to generator spacing; for a given configuration of vortex generators positioned at a fixed axial location, there exists a spacing angle which will minimize engine face distortion at a given flow condition.

Presented in Fig. 18 is a comparison between the vortex α_{vg} characteristics for a generator configuration optimized for both the test case 3.2 initial conditions and flight conditions, i.e., VG130 and VG430 series generator configurations, respectively. As with the other vortex generator parameters previously discussed, it is apparent that the choice of optimum α_{vg} (i.e., lateral distance between generator blades) is a more critical decision for an installation designed for a typical scaled wind-tunnel test environment than at flight Reynolds numbers. The spacing angle characteristics presented in Fig. 18 also reveal that there is a very limited set of lateral spacings between generator blades where scaling between flight and wind tunnel is even possible, and these spacings lie in the neighborhood of the optimum angle.

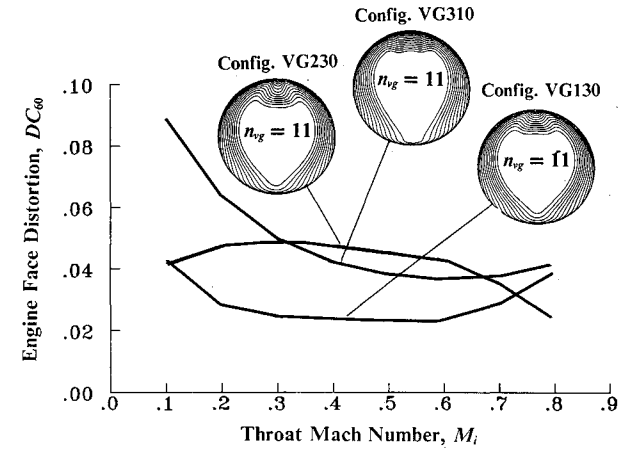

Fig. 19 Effect of vortex generator configuration on engine face DC_{60} distortion as a function of M_i, Pt_0 = 29.889 in./Hg, Tt_0 = 293 K.

Figure 19 presents the effect of vortex generator configuration on DC_{60} as a function of M_i, where Pt_0 and Tt_0 were held constant at the test case 3.1 values. The vortex generator installations include configurations VG130, VG230, and VG310, which have previously been defined. In general, minimum DC_{60} engine face distortion occurred at the conditions about which the generator installation was optimized. As the flow inlet throat Mach number moves away from the design throat Mach number, the performance of the generator installation degrades, i.e., the DC_{60} increases. The degree to which the performance degrades depends upon the geometry, arrangement, and placement of the generator installation within the inlet duct. In this example, the best overall performance over the Mach number range from 0.10 to 0.80 was achieved by the VG130 generator installation. The total pressure losses associated with these vortex generator configurations indicate a strong influence of blade height. At the test case 3.1 initial conditions, the total pressure losses $\Delta Pt/Pt_0$ were 0.005, 0.008, and 0.010, for configurations VG310, VG130, and VG230, respectively. These configurations correspond to h/R_i of 0.060, 0.075, and 0.080.

Perspective on Vortex Generator Design

Looking over the experimental work that has been done over the past few years to develop generator installations for inlet ducts, it is quite clear that the purpose of vortex generators for internal flow control is really to limit or minimize engine face distortion, particularly circumferential distortion. Although not explicitly stated as a goal, this is clearly what the development engineers had in mind in the re-engining of the 727-100 center inlet duct for the JT8D series engine.[3] As such, fundamental or even applied research ought to reflect this goal, and make a distinction between suppressing local flow separation (which is the external flow problem), and minimizing engine face distortion (which is the internal flow problem). Suppressing local flow separation is a necessary, but not a sufficient condition in the design of a vortex generator installation for inlet ducts. However, minimizing engine face distortion is both a necessary and sufficient condition for any internal flow management technique. Although these two goals are related, there are many examples where suppressing separation does not lead to a very good engine face distortion.

One such example is illustrated in Fig. 20, which presents C_f along the θ = 180-deg surface element of the M2129 inlet S-duct at the test case 3.2 initial conditions for three vortex generator configurations: 1) the baseline configuration, i.e., without vortex generators; 2) VG130n; and 3) VG130. VG130n has the same geometry, arrangement, and location as configuration VG130, except it has only one pair of corotating (or counter-rotating) generators, as compared to 11 pairs of co-

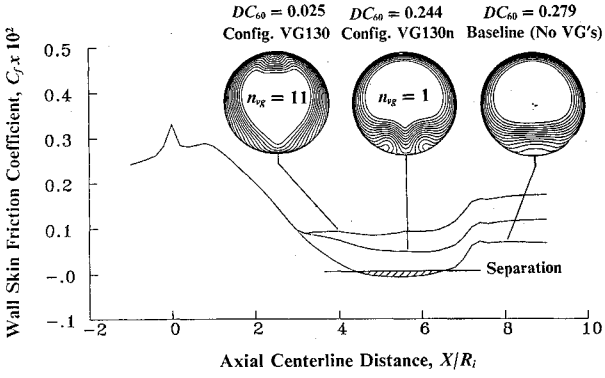

Fig. 20 Effect of vortex generator configuration on C_f along the θ = 180 deg surface element and test case 3.2 conditions.

rotating generators for configuration VG130. Also shown on Fig. 20 are the DC_{60} engine face distortion values for each of these configurations mentioned, as well as the engine face recovery maps. The baseline inlet duct (i.e., without vortex generators) separates, and this separation is indicated in Fig. 20 as a negative wall skin friction coefficient between the axial centerline stations X/R_i = 4.5 and X/R_i = 6.5. The computed DC_{60} was 0.279 for the baseline case. With the installation of one corotating generator pair, the separation within the M2129 inlet duct was eliminated as indicated by the positive wall skin friction distribution in Fig. 20. But this vortex generator configuration only reduced the DC_{60} distortion from 0.279 to 0.244. However, VG130 also eliminated the flow separation in the M2129 inlet S-duct, but it reduced the DC_{60} from 0.279 to 0.025. Therefore, the design problem is the control of secondary flow, not the elimination of local flow separation, and the rules for the design of vortex generator installation and the experimental studies used to understand the aerodynamics of vortex generators must reflect this goal.

Concluding Remarks

The present study demonstrates the capability of the RNS3D code to design a vortex generator system for the M2129 inlet S-duct, where the goal was to minimize inlet distortion by controlling secondary flow. The M2129 inlet duct, with the installed vortex generator system, will be tested over a wide range of flow conditions, including angle-of-incidence and angle-of-yaw. The experimental data thus generated will be used to validate the present vortex generator model, as well as future models, and will substantiate the concept of vortex flow control and its ability to manage inlet distortion. This research study also established the nature of the performance improvements that can be realized with vortex flow control, and suggests a set of aerodynamic properties (called observations) that can be used to arrive at a successful vortex generator installation design. The ultimate aim of this research is to manage inlet distortion by controlling secondary flow through arrangements of vortex generators configurations tailored to the specific aerodynamic characteristics of the inlet duct. This study also indicated that scaling between flight and typical wind-tunnel test conditions is possible only within a very narrow range of generator configurations close to an optimum installation. Lastly, this study indicated that vortex generator installation design for inlet ducts is more complex than simply satisfying the requirement of attached flow, it must satisfy the requirement of minimum engine face distortion.

References

[1]Advisory Group for Aerospace Research and Development (AGARD), "Engine Response to Distorted Inflow Conditions," AGARD CP-400, Munich, Germany, Sept. 1986.

[2]Bowditch, D. N., and Coltrin, R. E., "A Survey of Inlet/Engine Distortion Compatability," AIAA Paper 83-1166, June 1983.

[3]Kaldschmidt, G., Syltedo, B. E., and Ting, C. T., "727 Airplane Center Duct Inlet Low-Speed Performance Confirmation Model Test for Refanned JT8D Engines—Phase II," NASA CR-134534, Nov. 1973.

[4]Briley, W. R., and McDonald, H., "Analysis and Computation of Viscous Subsonic Primary and Secondary Flow," AIAA Paper 79-1453, Jan. 1979.

[5]Briley, W. R., and McDonald, H., "Three-Dimensional Viscous Flows with Large Secondary Velocities," *Journal of Fluid Mechanics*, Vol. 144, March 1984, pp. 47–77.

[6]Levy, R., Briley, W. R., and McDonald, H., "Viscous Primary/Secondary Flow Analysis for Use with Nonorthogonal Coordinate Systems," AIAA Paper 83-0556, Jan. 1983.

[7]Anderson, B. H., "The Aerodynamic Characteristics of Vortex Ingestion for the F/A-18 Inlet Duct," AIAA Paper 91-0130, Jan. 1991.

[8]McDonald, H., and Camarata, F. J., "An Extended Mixing Length for Computing the Turbulent Boundary-Layer Development, Proceedings, Stanford Conference of Turbulent Boundary Layers," Vol. I, Stanford Univ., Stanford, CA, 1969, pp. 83–98.

[9]Squire, R., "Growth of a Vortex in Turbulent Flow," *Aeronautical Quarterly*, Vol. 16, Pt. 3, Aug. 1965, pp. 302–306.

[10]Anderson, B. H., and Farokhi, S., "A Study of Three Dimensional Turbulent Boundary Layer Separation and Vortex Flow Control Using the Reduced Navier Stokes Equations," Turbulent Shear Flow Symposium, Univ. of Munich, Munich, Germany, Sept. 1991.

[11]Willmer, A. C., Brown, T. W., and Goldsmith, E. L., "Effects of Intake Geometry on Circular Pitot Intake Performance at Zero and Low Forward Speeds," *Aerodynamics of Power Plant Installation*, AGARD CP301, Paper 5, Toulouse, France, May 1981, pp. 5-1–5-16.

[12]Pearcy, H. H., "Shock Induced Separation and Its Prevention," *Boundary Layer and Flow Control*, edited by G. V. Lachmann, Vol. 2, Pergamon, Oxford, England, UK, 1961, pp. 1166–1355.